

NSVS 07394765: A new low-mass eclipsing binary below $0.6 M_{\odot}$

Ömür Çakırlı^{a,*}

^a*Ege University, Science Faculty, Astronomy and Space Sciences Dept., 35100 Bornova,
İzmir, Turkey.*

Abstract

The multi-color photometric and spectroscopic¹ observations of the newly discovered eclipsing binary NSVS 07394765 were obtained. The resultant light and radial velocities were analysed and the global parameters of the system: $T_1=3\,300\text{ K}$; $T_2=3\,106\text{ K}$; $M_1=0.36 M_{\odot}$; $M_2=0.18 M_{\odot}$; $R_1=0.46 R_{\odot}$; $R_2=0.50 R_{\odot}$; $L_1=0.030 L_{\odot}$; $L_2=0.026 L_{\odot}$; $i = 89.2^{\circ}$; $a = 5.97 R_{\odot}$; $d = 28\text{ pc}$. The chromospheric activity of its components is revealed by strong emission in the $H\alpha$ line and observed flares. Empirical relations for mass-radius and mass-temperature are derived on the basis of the parameters of known binaries with low-mass dM components.

Keywords: Binaries Eclipsing – stars: fundamental parameters Individual method:spectroscopy

*Corresponding author

Email address: omur.cakirli@gmail.com, Tel:+90 (232) 3111740, Fax:+90 (232) 3731403 (Ömür Çakırlı)

¹Based on observations obtained with the TÜBİTAK National Observatory 1.5-meter telescope, which is owned and operated by the TÜBİTAK.

1. Introduction

The M dwarfs are the most numerous stars in our Galaxy. They are quite poorly investigated because of the selection effect. The values of masses, radii, luminosities and temperatures are less than those of 30 binaries with low-mass eclipsing binary components given by (Cakirli, İbanoglu & Sipahi, 2012). The mass-temperature and temperature-radii relation is determined by only a few low-mass stars. This situation has prevented the development of the models for the M dwarfs. It is created that all available models underestimate the radii (by around 10-15 per cent) and overestimate the temperatures (by 200-300 K) of short and long period binaries with M components (Cakirli, İbanoglu & Sipahi, 2012).

The Northern Sky Variability Survey (NSVS) contains a great number of photometric data (Wozniak et al., 2004) that allows searching of variable stars and determination of their periods and types of variability. One of them was NSVS 07394765 \equiv 2MASS J082551+242725 ($\alpha=08^h25^m51^s.3$, $\delta=+24^\circ27'05''.1$).

On the base of the NSVS photometry obtained in 1999–2000 we derived the ephemeris: $\text{HJD}(\text{MinI})=2451503.363 + 2.2656 \times E$ and built its light curve (Fig. 1).

Initially NSVS 07394765 attracted our interest by its very active components because there were only several systems with non-degenerate components and periods above the long-period limit of 4.26 days (Cakirli, İbanoglu & Sipahi, 2012): CU Cnc (Ribas, 2003) with $P = 2.794$ d, 2MASS J01542930+0053266 (Becker et al., 2008) with $P = 2.619$ d, and T-Cyg1-12664 (Cakirli, İbanoglu & Sipahi, 2012) with $P = 4.2631$ d.

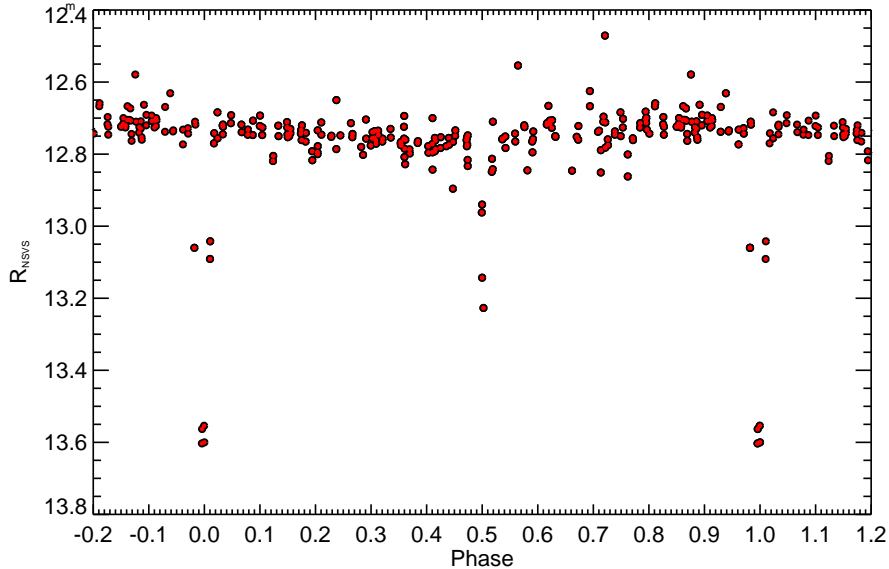


Figure 1: NSVS photometry of NSVS 07394765.

When we determined that the components of NSVS 07394765 were low-mass eclipsing binary our interest increased and we undertook intensive photometric and spectral observations in order to determine its global parameters and to add a new information for the low-mass stars as well as for the very active and binary masses between $0.2\text{-}0.4 M_{\odot}$.

2. Observations and data reduction

2.1. Photometry

NSVS 07394765 was first identified in the NORTHERN SKY VARIABILITY SURVEY (NSVS; Wozniak et al. 2004) as a detached eclipsing binary system with a maximum, out-of-eclipse V-bandpass magnitude $R=12^m.75$ and a period of $P = 2.2656$ d. The data from the NSVS, obtained with the

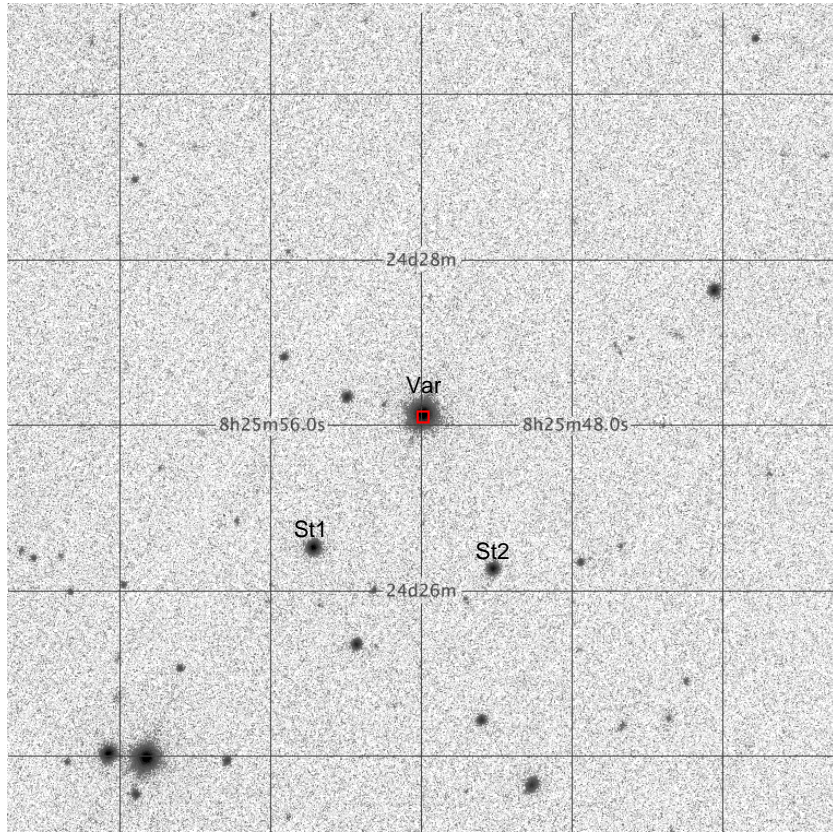


Figure 2: Observed field around NSVS 07394765.

Robotic Optical Transient Search Experiment telescopes (ROTSE), contains positions, light curves and V magnitudes for about 14 million objects ranging in magnitudes from 8 to 15.5.

The B, V, R, and I magnitudes for NSVS 07394765 were listed in the USNO NOMAD catalog as (NAVAL OBSERVATORY MERGED ASTRONOMICAL DATASET, NOMAD-1.0, (Zacharias, Monet & Levine, 2004), B= $14^m.35$, V= $13^m.9$, R= $11^m.42$ and I= $11^m.22$; on the other hand the infra-red magnitudes in three bandpasses were given as J= $10^m.554$, H= $9^m.880$ and K= $9^m.720$ in the 2MASS catalog (Cutri et al. , 2003).

The photometric observations of NSVS 07394765 were carried out with the 0.4 m telescope at the Ege University Observatory. The 0.4 m telescope equipped with an Apogee CCD camera and standard Bessel BVRI bandpasses. The observations were performed on five nights between February 01 and March 30, 2009. To get the higher accuracy the target NSVS 07394765 was placed near to the center of the CCD and three nearby stars located on the same frame were taken for comparison. The field of the variable and standard stars is shown in Fig. 2. The stars TYC 1941-1874-1 and HD 70897 were selected as comparison and check, respectively. Therefore the target and comparison stars could be observed simultaneously with an exposure time of 10 seconds. The differential observations of the comparison stars showed that they are stable during time span of our observations. The data were processed with standard data reduction procedures including bias and over scan subtraction, flat-fielding, and aperture photometry. The average uncertainty of each differential measurement was less than $0^m.030$. The B-, V-, R- and I-bandpass magnitude differences, in the sense of variable minus comparison,

Table 1: Differential photometric measurements of NSVS 07394765 in the B, V, R and I bandpasses.

HJD(2 400 000+)	ΔB	HJD(2 400 000+)	ΔV	HJD(2 400 000+)	ΔR	HJD(2 400 000+)	ΔI
54520.53155	1.214	54520.52299	0.659	54520.53481	0.259	54520.51694	-0.179
54520.53283	1.220	54520.52428	0.647	54520.53610	0.282	54520.51823	-0.185
...
...

are listed in Table 1 (available in the electronic form at the CDS).

The light curve shows a deep primary eclipse with an amount of $0^m.85$ in the V-bandpass and a shallow secondary eclipse with an amount of $0^m.45$ which are clearly separated in phase, as is typical of fully detached binaries. The primary and secondary eclipses occur almost 0.5 phase interval, indicating nearly circular orbit. An inspection of the nightly light curves presented in Fig. 3 clearly indicates considerable out-of-eclipse light variations up to $0^m.2$. This intrinsic variation of the binary system manifests itself in the deeper primary eclipse.

2.1.1. *Orbital period and ephemeris*

The first orbital period for NSVS 07394765 was determined as $P = 2.2656$ d by Wozniak et al. (2004) from the NSVS database. Later on Coughlin & Shaw (2007) observed seven low-mass detached systems, including NSVS 07394765. An orbital period and an initial epoch for the mid-primary eclipse were calculated using a least square fit. Partial primary and secondary eclipses which were detected in the time series photometric data were used in combination with the NSVS photometry to derive this ephemeris for the system.

We obtained a time of mid-primary and secondary eclipse during our observing run. The mid-eclipse timings and their standard deviations are

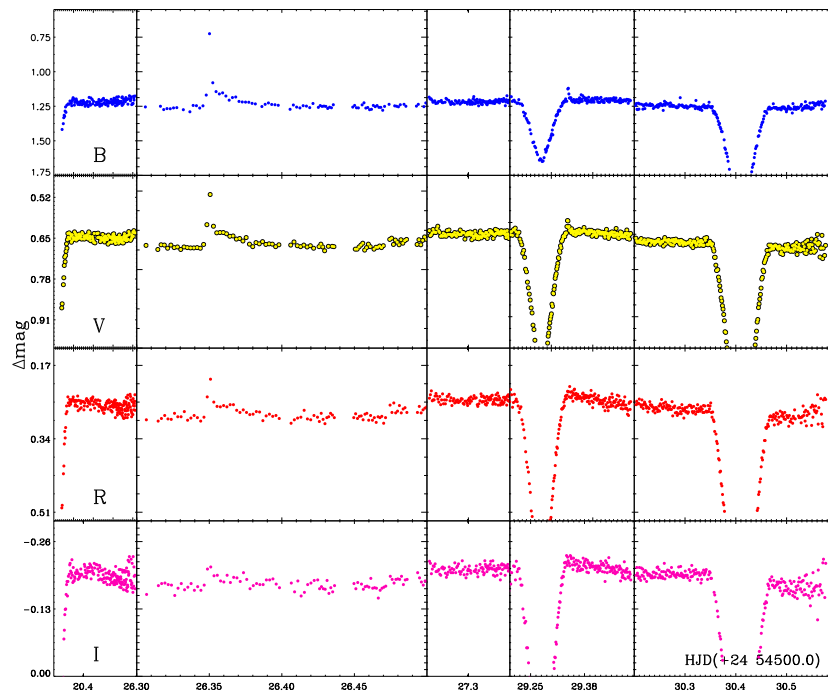


Figure 3: The B-, V-, R-, and I-bandpass nightly light curves for NSVS 07394765 from top to bottom. The B-, V-, R-, and I-bandpass light curves clearly show that the brightness of the variable significantly varies from night to night, particularly in out of eclipse.

calculated using the method of Kwee & van Woerden (1956). These timings of the eclipses were listed in Table 2 together with three primary and two secondary eclipses collected from literature. The times for mid-eclipses are the average of times obtained in four bandpasses. We define the epoch of the system, T_0 , to be the midpoint of the most complete primary eclipse. For this reason we use the B-, V-, R-, and I-bandpass data obtained on JD=2 454 530 which cover almost the whole primary eclipse. A linear least square fit to the data listed in Table 2 yields the new ephemeris as,

$$\text{Min } I(HJD) = 24\,54530.4143(5) + 2.265754(11) \times E, \quad (1)$$

where E corresponds to the cycle number. The residuals in the last column of Table 2 are computed with the new ephemeris. While the orbital period is nearly the same with that determined by Coughlin & Shaw (2007) its uncertainty is now very smaller than estimated by them. In the computation of the orbital phase for individual observations we used this ephemeris.

2.2. Spectroscopy

Optical spectroscopic observations of the NSVS 07394765 were obtained with the Turkish Faint Object Spectrograph Camera (TFOSC)² attached to the 1.5 m telescope in January, 2012, under good seeing conditions. The wavelength coverage of each spectrum was 4000-9000 Å in 12 orders, with a resolving power of $\lambda/\Delta\lambda \sim 7000$ at 6563 Å and an average signal-to-noise ratio (S/N) was ~ 120 . We also obtained high S/N spectra of two M dwarfs

²http://tug.tug.tubitak.gov.tr/rtt150_tfosc.php

Table 2: Times of minima of system.

HJD(2 400 000+)	E	Type	O-C
51503.3625**	-1336.0	I	-0.0049
51511.2973**	-1332.5	II	-0.0003
51553.1954**	-1314.0	I	-0.0186
51579.2599**	-1302.5	II	-0.0103
53730.7303 [†]	-353.0	I	0.1271
54529.2761±0.0005	-0.5	II	-0.0053
54530.4094±0.0001	0.0	I	-0.0049

** From the NSVS database

[†] Coughlin & Shaw (2007)

GJ 740 (M0 V) and α Cet (M1.5 III) for use as templates in derivation of the radial velocities.

3. Analysis

3.1. Effective temperature of the primary star

We have used our spectra to reveal the spectral type of the primary component of NSVS 07394765. For this purpose we have degraded the spectral resolution from 7 000 to 3 000, by convolving them with a Gaussian kernel of the appropriate width, and we have measured the equivalent widths of photospheric absorption lines for the spectral classification. We have followed the procedures of Hernández et al. (2004), choosing helium lines in the blue-wavelength region, where the contribution of the secondary compo-

ment to the observed spectrum is almost negligible. From several spectra we measured $EW_{\text{HeI}+\text{FeI}\lambda 4922} = 0.98 \pm 0.09 \text{ \AA}$, $EW_{\text{MgI}\lambda 5711} = 0.54 \pm 0.08 \text{ \AA}$ and $EW_{\text{TiII}+\text{FeII}\lambda 4203} = 1.38 \pm 0.11 \text{ \AA}$. From the calibration relations EW -Spectral-type of Hernández et al. (2004), we have derived a spectral type of M2 with an uncertainty of about 1 spectral subclass.

The effective temperature deduced from the calibrations of Drilling & Landolt (2000), de Jager & Nieuwenhuijzen (1987), Alonso et al. (1996), Flower (1996) and Popper (1980) and Straizys & Kuriliene (1981) are $3300 \pm 90 \text{ K}$, $3488 \pm 150 \text{ K}$, $3382 \pm 180 \text{ K}$, $3060 \pm 150 \text{ K}$, $3100 \pm 300 \text{ K}$ and $3050 \pm 100 \text{ K}$, respectively. The standard deviations were estimated from the spectral-type uncertainty. The weighted mean of the effective temperature was obtained for the primary star as $3300 \pm 130 \text{ K}$.

Taking into account that $E(V - I) = 0.013$, mag in the NSVS 07394765 direction (Schlafly & Finkbeiner, 2011), we obtained its de-reddened color index $(V - I)_0 = 2.67$ mag. According to the table 2 of Vandenberg & Clem (2003), this out-of-eclipse color index corresponds to a mean temperature of the binary $T_m = 3400 \text{ K}$.

The catalogs USNO, NOMAD and GSC2.3 provide BVRIJHK magnitudes for NSVS 07394765 with a few tenths of a magnitude uncertainties. Using the USNO B-mag of 14.35 ± 0.20 and V-mag of 13.9 ± 0.3 we obtained an observed color of $B - V = 0.45 \pm 0.36$ mag. The observed infrared colors of $J - H = 0.674 \pm 0.021$ and $H - K = 0.160 \pm 0.021$ are obtained using the JHK magnitudes given in the 2MASS catalog (Cutri et al. , 2003). These colors correspond to a main-sequence $M1 \pm 2$ star which is consistent with that estimated from the spectra.

3.2. Radial velocity

To derive the radial velocities of the components, the 12 TFOSC spectra of the eclipsing binary were cross-correlated against the spectrum of GJ 740, a single-lined M0 V star, on an order-by-order basis using the FXCOR package in IRAF. The majority of the spectra showed two distinct cross-correlation peaks in the quadrature, one for each component of the binary.

The heliocentric radial velocities for the primary (V_p) and the secondary (V_s) components are listed in Table 3, along with the dates of observations and the corresponding orbital phases computed with the new ephemeris given in previous section. The radial velocities are plotted against the orbital phase in Fig. 4.

First we analysed the radial velocities for the initial orbital parameters. We used the orbital period held fixed and computed the eccentricity of the orbit, systemic velocity and semi-amplitudes of the radial velocities. The results of the analysis are as follows: $e=0.001\pm 0.001$, i.e. formally consistent with a circular orbit, $\gamma=12\pm 1$ km s⁻¹, $K_1=44\pm 3$ and $K_2=88\pm 4$ km s⁻¹. Using these values we estimate the projected orbital semi-major axis and mass ratio as: $a\sin i=5.97\pm 0.51 R_\odot$ and $q = \frac{M_2}{M_1}=0.505\pm 0.009$

3.3. Light curve modeling

We used the most recent version of the eclipsing binary light curve modeling algorithm of Wilson & Devinney (1971), as implemented in the PHOEBE code of Prša & Zwitter (2005). The code needs some input parameters, which depend upon the physical properties of the component stars.

The BVRI photometric observations were analyzed simultaneously. The adjustable parameters in the light curves fitting were the orbital inclination,

Table 3: Heliocentric radial velocities of NSVS 07394765. The columns give the heliocentric Julian date, the orbital phase (according to the ephemeris in Eq. 1), the radial velocities of the two components with the corresponding standard deviations.

HJD 2400000+	Phase	Star 1		Star 2	
		V_p	σ	V_s	σ
55929.55435	0.5163	11.1	8.8	—	—
55929.64995	0.5585	19.9	8.7	-25.5	9.8
55930.42082	0.8987	25.6	4.4	-51.2	11.1
55930.46351	0.9176	17.8	11.1	-41.1	12.2
55930.55057	0.9560	14.3	10.9	—	—
55930.64022	0.9956	10.0	8.8	—	—
55931.25253	0.2658	-22.2	3.5	99.9	6.7
55931.39789	0.3300	-18.2	4.3	88.4	5.4
55931.44056	0.3488	-17.3	4.3	81.1	9.8
55931.48835	0.3699	-13.3	4.4	77.7	7.8
55932.37000	0.7590	37.4	5.2	-88.7	6.5
55932.49211	0.8129	33.3	3.2	-82.1	7.4

Table 4: Results of the our ground-based BVRI light curves analyses for NSVS 07394765.

Parameters	<i>BVRI</i>
i°	89.23 ± 0.03
T_{eff1} (K)	3300[Fix]
T_{eff2} (K)	3106 ± 2
Ω_1	13.595 ± 0.051
Ω_2	7.110 ± 0.019
r_1	0.0768 ± 0.0003
r_2	0.0861 ± 0.0003
$\frac{L_1}{(L_1+L_2)}$	$0.582 \pm 0.003; 0.562 \pm 0.002; 0.541 \pm 0.002; 0.522 \pm 0.003$
χ^2	0.9635
Spot1	Primary
Latitude (deg)	145
Longitude (deg)	290
Angular radius (deg)	20
$T_{spot}/T_{photosphere}$	0.89
Spot2	Primary
Latitude (deg)	90
Longitude (deg)	360
Angular radius (deg)	18
$T_{spot}/T_{photosphere}$	0.92

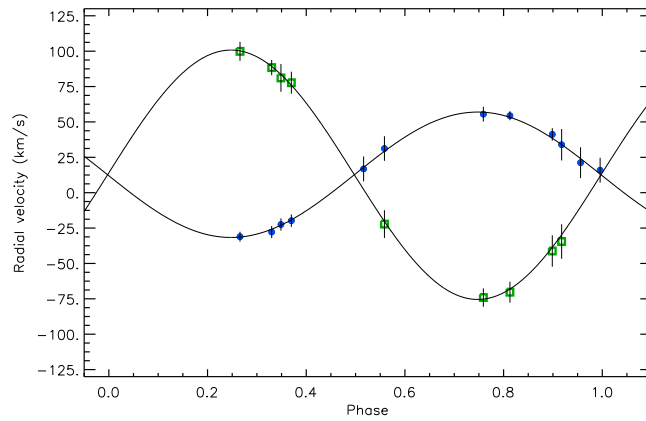


Figure 4: Radial velocities folded on a period of 2.2656-day and the model. Points with error bars (error bars are masked by the symbol size in some cases) show the radial velocity measurements for the components of the system (primary: filled circles, secondary: open squares).

the surface potentials, the effective temperature of secondary, and the luminosity of the hotter star. Our final results are listed in Table 4 and the computed light curves (continuous line) are compared with the observations in Fig. 5. The uncertainties assigned to the adjusted parameters are the internal errors provided directly by the Wilson-Devinney code. The distortions at out-of-eclipses are clearly seen in the BVRI light curves. Therefore wave-like distortions are taken into account in the analysis of the BVRI light curves.

4. Global parameters of the NSVS 07394765

The weighted mean of the orbital inclination and fractional radii of the components are found to be $i=89.23\pm 0.03$, $r_1=0.0768\pm 0.0003$, and $r_2=0.0861\pm 0.0003$ from the light curves analyses. Using the orbital inclination and the semi-amplitudes of the radial velocities we determine the separation between the components as $a=5.973\pm 0.510 R_\odot$. For the de-reddening, we used the $E(B-V) = 0.009$ value from Schlafly & Finkbeiner (2011). The interstellar reddening yield a distance to the system as 28 ± 3 pc for the bolometric correction of -1.89 mag for a M2 main-sequence star (Drilling & Landolt, 2000). The effective temperature of 5770 K and bolometric magnitude of 4.74 mag are adopted for the sun. The standard deviations of the parameters have been determined by JKTABSDIM³ code, which calculates distance and other physical parameters using several different sources of bolometric corrections (Southworth et al. 2005). The best fitting parameters are listed in Table 5 together with their formal standard deviations.

³This can be obtained from <http://http://www.astro.keele.ac.uk/~jkt/codes.html>

Table 5: Fundamental parameters of NSVS 07394765.

NSVS 07394765		
Parameter	Primary	Secondary
Mass (M_{\odot})	0.360 ± 0.005	0.180 ± 0.004
Radius (R_{\odot})	0.463 ± 0.004	0.496 ± 0.005
T_{eff} (K)	$3\,300 \pm 200$	$3\,106 \pm 125$
$\log g$ (<i>cgs</i>)	4.664 ± 0.006	4.302 ± 0.009
$\log (L/L_{\odot})$	-1.53 ± 0.06	-1.59 ± 0.08
$(v \sin i)_{calc.}$ (km s^{-1})	10 ± 1	11 ± 1
Spectral Type	M2V ± 1	M4V ± 1
a (R_{\odot})	5.973 ± 0.510	
V_{γ} (km s^{-1})	12 ± 1	
i ($^{\circ}$)	89.23 ± 0.03	
q	0.5049 ± 0.0088	
d (pc)	28 ± 3	
$\mu_{\alpha} \cos \delta, \mu_{\delta}$ (mas yr^{-1})	$8 \pm 3, 48 \pm 5$	
U_o, V_o, W_o (km s^{-1})	$-2 \pm 1, 15 \pm 1, 15 \pm 1$	

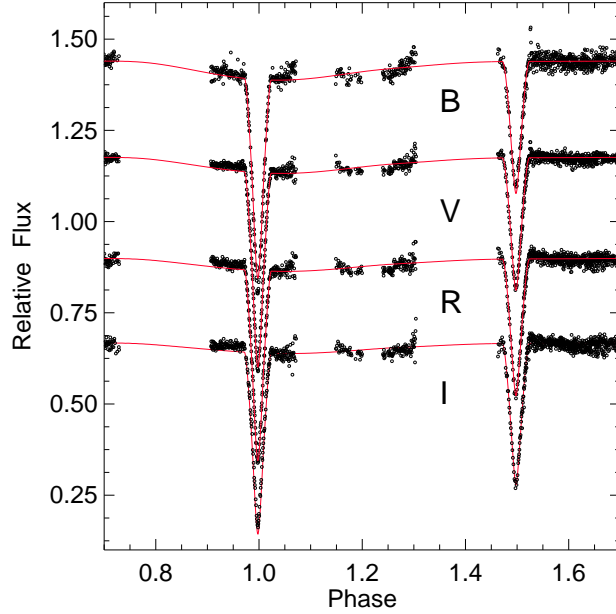


Figure 5: The observed and computed light curves of NSVS 07394765.

4.1. Kinematics

To study the kinematical properties of NSVS 07394765, we used the system’s centre-of-mass velocity, distance and proper motion values, which are given in Table 5. The proper motion data were taken from 2MASS catalogue (Cutri et al. , 2003), whereas the centre-of-mass velocity and distance are obtained in this study. The system’s space velocity was calculated using Johnson & Soderbloms (1987) algorithm. The U, V and W space velocity components and their errors were obtained and given in Table 5. To obtain the space velocity precisely, the first-order galactic differential rotation correction was taken into account (Mihalas & Binney, 1981), and -1.08 and 0.65 km s^{-1} differential corrections were applied to U and V space velocity components, respectively. The W velocity is not affected in this first-

order approximation. As for the LSR (Local Standard of Rest) correction, Mihalas & Binney (1981) values $(9, 12, 7)_{\odot}$ km s⁻¹ were used and the final space velocity of NSVS 07394765 was obtained as $S=21$ km s⁻¹. This value is in agreement with space velocities of the young stars.

5. Activity of NSVS 07394765

The H α emission lines from the system is an useful indicator of chromospheric activity for late-type stars, in particularly M dwarfs. Typically, M dwarfs are divided into 4 subsets by Stauffer & Hartmann (1986) in conformity with the strength of chromospheric activity. The lowest degree of chromospheric active M dwarfs have feeble H α absorption line in a spectrum. As the chromosphere increases the equivalent width of the H α absorption increases, then reducing and finally H α goes into the emission.

H α emission from the NSVS 07394765 was present in every observed spectrum, as shown in Fig. 6 as a function of the selected orbital phase. This is usual property of M dwarfs in general, because of the magnetic activity is frequently characterized by strong and variable H α line emission. Emission line characteristic varies with M dwarfs age, spectral type (particularly M2 or later), and the lifetime of magnetic activity (West et al., 2011; Bell et al., 2012). Like this variety also seen from the M dwarfs in close binary systems with other dwarf stars (e.g. Dimitrov & Kjurkchieva, 2010).

We measured the H α equivalent width for each spectra and investigated variety of the strength of emissions. Although it seemed to change unusually in the range 3.2-4.4 Å with orbital phase we noted a trend of the equivalent width to be higher level of H α equivalent width at conjuncture.

The $H\alpha$ structure was observed to be broader and stronger than other activity indicators line (e.g. Ca I absorption lines and $H\beta$ emission lines). Comparison of the structure with some binaries with low-mass M components from the Cakirli, İbanoglu & Sipahi (2012) reveals the strong $H\alpha$ emission of the system. This conclusion is not surprising taking into account the low temperature and fast rotation of its components. The mean value equivalent width 4 \AA of the $H\alpha$ emission of NSVS 07394765 is considerably smaller than that of the accreting pre-main sequence dMe stars which $H\alpha$ emission width has greater than ten angstrom.

Besides the variability of the line profiles there is information about optical flares of the system in the obtained photometrical data. Generally, flare activity is typical for late-type stars. Until recently, the active M dwarfs in close binary system in the literature was CM Dra, V405 And, YY Gem and GSC 2314-0530 (e.g. Dimitrov & Kjurkchieva, 2010). It should be noted that 2 observed flares occurred around the HJD 54526.35 and 54529.31. This involves correlation between the two signs of stellar activity: spots and flares. Both of them are appearances of the long-lived active area on the components.

No other demonstrative clues for accretion, or outflow in the form of emission structure was observed. It does not appear that the $H\alpha$ emission is partially coming from the third body or other physical processes, but more likely from many distributed active region on both stars. Longer duration and higher resolution spectroscopic monitoring would be necessary to accurately determine the geometry of the $H\alpha$ emission regions, and the active region timescales.

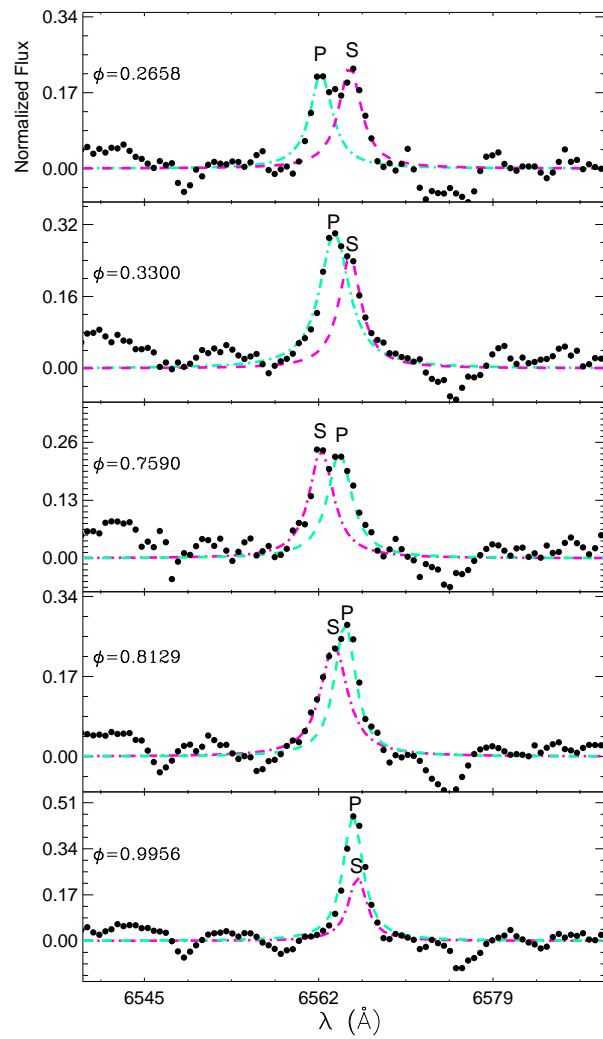


Figure 6: Echelle spectra of H α lines are shown at several phases. Dashed lines shows the resulting fit of Gaussians to the line profile with letters indicating each component.

6. Conclusions

The analysis of our photometric and spectral observations of the eclipsing binary NSVS 07394765 allows us to derive the following conclusions:

We have presented follow up photometric and first time spectroscopic observations of a low-mass binary, NSVS 07394765, whose total mass of the components are below the limit of full convection dwarfs. The components of the system have masses typical M2 and M4, are in detached configuration.

By simultaneous radial velocity solution and light curve solution we determined the global parameters of the system described in §4 and showed in Table 5.

In Fig. 7 we derived empirical positions of the NSVS 07394765 components in the mass-radius (M-R) and mass - effective temperatures (M- T_{eff}) planes relative to those of the well-determined low-mass dM components in the eclipsing binary systems. Theoretical M-R diagrams for a zero-age main-sequence stars with $[M/H]=0$ taken from the Baraffe et al. (1998) are also plotted to comparison. Due to the high magnetic activity in the fast-rotating dwarfs their surfaces are covered by dark spot(s) or spot groups. Spot coverage in active dwarfs yields larger radii and lower effective temperatures.

The distorted light curve of NSVS 07394765 were reproduced by two cool spots on the primary component. The next sign of the activity of the system is the strong $H\alpha$ emission of its components. Moreover we registered 2 flares of NSVS 07394765. Both of them occurred at the phases of maximum visibility of the larger stable cool spot on the primary.

The analysis of all appearances of magnetic activity revealed existence of long-lived active area on the primary of the system. The high activity of the

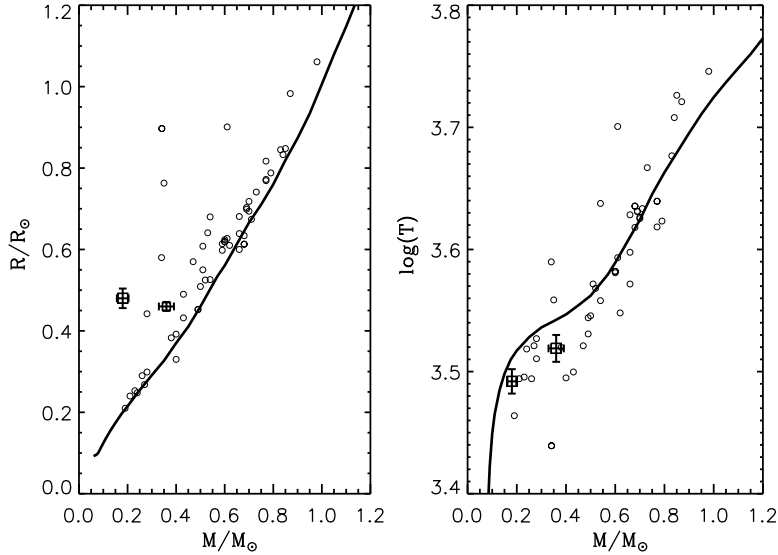


Figure 7: Components of NSVS 07394765 (squares with error bars) in the mass-radius plane (left panel). The less massive component is located among the most deviated stars from the theoretical mass-radius relationship Cakirli, İbanoglu & Sipahi (2012). The lines show stellar evolution models from Baraffe et al. (1998) for zero-age main-sequence with $[M/H]=0$ (solid line). Components of the system (squares with error bars) in the mass-effective temperature plane (right panel).

target is natural consequence of the fast rotation and low temperatures of its components.

Our study on one of the lowest-mass eclipsing binary NSVS 07394765 presents a next small step toward understanding dMe stars and adds a new information to the poor statistic of the low-mass dM stars. Recently they became especially interesting as appropriate targets for planet searches due to the relative larger transit depths.

Acknowledgments

We thank to TÜBİTAK National Observatory (TUG) for a partial support in using RTT150 and T100 telescopes with project numbers 10ARTT150-483-0, 11ARTT150-123-0 and 10CT100-101. We also thank to the staff of the Bakırtepe observing station for their warm hospitality. The following internet-based resources were used in research for this paper: the NASA Astrophysics Data System; the SIMBAD database operated at CDS, Strasbourg, France; TÜBİTAK ULAKBİM Süreli Yayınlar Kataloğu-TURKEY; and the arXiv scientific paper preprint service operated by Cornell University.

References

- Alonso, A., Arribas S., and Martinez-Roger, C., 1996, AA, 313, 873
- Baraffe I., Chabrier G., Allard F., Hauschildt P., 1998, A&A, 337, 403
- Becker A. et al., 2008, MNRAS, 386, 416
- Bell, K. J., Hilton, E. J., Davenport, J. R. A., Hawley, S. L., West, A. A., & Rogel, A. B. 2012, PASP
- Cakirli O., İbanoglu C., & Sipahi S., 2012, MNRAS, in press
- Coughlin J., Shaw J., 2007, J. of Southeastern Assoc. for Res. in Astr., 1, 7
- Cutri R. M., et al., 2003, The IRSA *2MASS* All-Sky Point Source Catalog, NASA/IPAC Infrared Science Archive. <http://irsa.ipac.caltech.edu/applications/Gator/>

- Drilling J. S., Landolt A. U., 2000, Allen's astrophysical quantities, 4th ed.
Edited by Arthur N. Cox. ISBN: 0-387-98746-0. Publisher: New York: AIP
Press; Springer, 2000, p.381
- Dimitrov, D. P., & Kjurkchieva, D. P. 2010, MNRAS, 406, 2559
- Flower P. J., 1996, ApJ, 469, 355
- Hernández J., Calvet N., Briceño C., Hartmann L., Berlind P., 2004, AJ,
127, 1682
- Johnson, D. R. H., & Soderbloms, D. R., 1987, AJ, 93, 864
- de Jager C., Nieuwenhuijzen H., 1987, AA, 177, 217
- Kwee K. K. & van Woerden H., 1956, BAN, 12, 327
- Mihalas, D., & Binney, J., 1981. in Galactic Astronomy, 2nd edition, Free-
man, San Fransisco, p.181
- Mullan D. J., MacDonald J., 2001, ApJ, 559, 353
- Prša A., Zwitter T., 2005, ApJ, 628, 426
- Popper D. M., 1980, Ann. Rev. AA, 18, 115
- Straizys V., Kuriliene G., 1981, Ap&SS, 80, 353
- Southworth J., Smalley B., Maxted P. F. L., Claret A. & Etzel P. B. 2005,
MNRAS, 363, 529
- Ribas I., 2003, A&A, 398, 239

Schlafly E. F., Finkbeiner D. P., 2011, ApJ, 737, 103

Stauffer J.R., Hartmann L.W., 1986, ApJS, 61, 531

West, A. A., et al. 2011, AJ, 141, 97

Wilson R.E. & Devinney E.J., 1971, ApJ, 166, 605

Wozniak P.R., Vestrand C.W., Akerlof R., et al., 2004, AJ, 127, 2436

VandenBerg D. A., Clem J. L., 2003, AJ, 126, 778

Zacharias N., Monet D. G., Levine S. E., 2004, AAS, 205, 4815Z